MESOSCALE MODELING OF COLD SPRAYED MULTI-PARTICLE IMPACT OF TANTALUM POWDERS

Ching Chen, Sumit Suresh, Avinash M. Dongare

Materials Science and Engineering, and Institute of Materials Science, University of Connecticut, Storrs, CT 06269, USA

Introduction

- Understanding the jetting and recrystallization behaviors in practical cold spray process require accurate description of microstructure evolution during high strain rate impact deformation.
- Such information can be obtained by atomistic modeling of multi-particle impact at length (micron) and time (nanosecond) scales of cold spray.
- Classical molecular dynamics (MD) simulation cannot be used directly for modeling multi-particle impact of cold spray due to its restrictions on system size and time scale.
- "Quasi-Coarse-Grained Dynamics" can extend the capability of MD simulation to mesoscale for modeling cold spray systems [1].

Quasi-Coarse-Grained Dynamics (QCGD) [1]

- N atoms in molecular dynamics (MD) simulation with a timestep t can be represented as N/A_{cg}^3 R-atoms in Level A_{cg} QCGD with a increased timestep $A_{cg}t$, accompanying with the scaling of interatomic potentials.
- The decrease in number of particles and the increase of timestep result in the reduction of computational workload, which allow QCGD to extend the capability of MD simulation to the mesoscale.

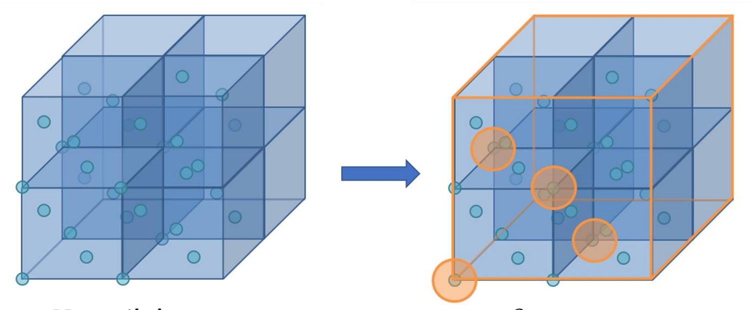

N particles N/A_{cg}^3 R-particles

Energy

$$E_i^R = \frac{1}{2}\sum_{j \neq i} \varphi_{ij}\left(\frac{r_{ij}^R}{A_{cg}}\right) + F_i\left[\sum_{j \neq i} f_j\left(\frac{r_{ij}^R}{A_{cg}}\right)\right]$$

Computational details

- Interactions is defined by **Ravelo's EAM** interatomic potential [2].
- System configuration: The system of current work is the continuation of a single particle impact simulation where a 20 um Tantalum polycrystalline powder with grain size of 10 um was impacted onto a 50 µm × 50 µm × 50 µm polycrystalline Tantalum substrate at a speed of 850 m/s. The second particle is a replica of the first particle which is equilibrated at 300 K and with the same impact velocity of 850 m/s. The types of second particle impacts include top and offset impact as shown in Figure 1 (a, b).
- System size: the system contains ~10^{16} atoms which are represented by using **~ 54 million R-atoms** in an **L512-QCGD** setup.

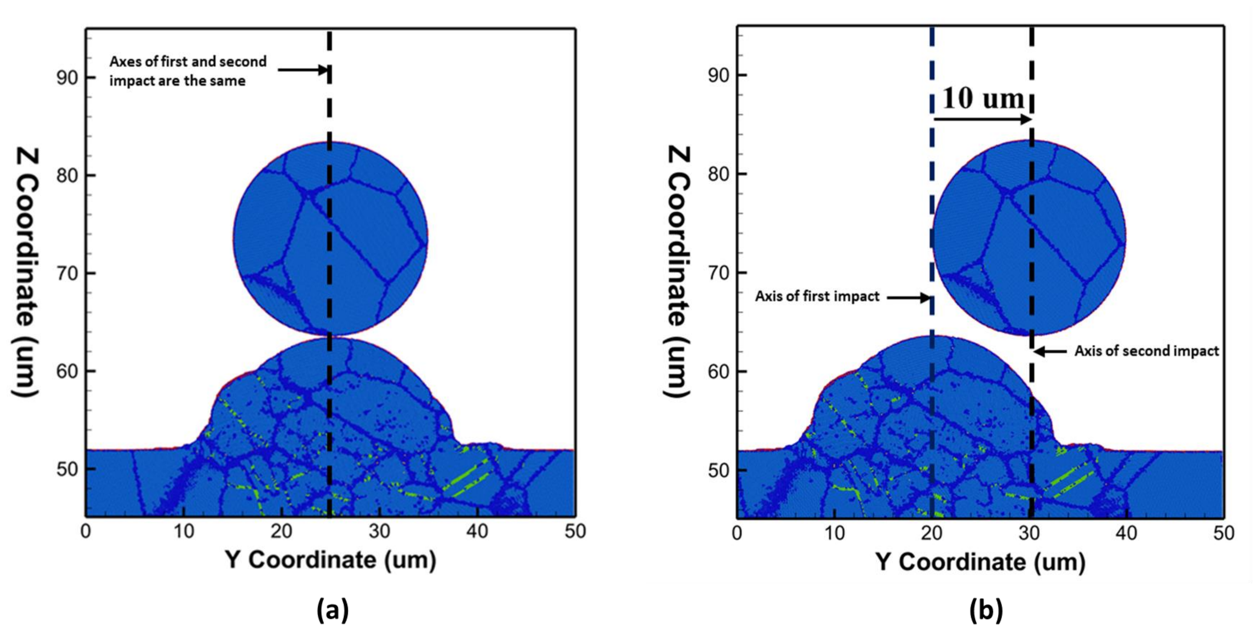

Figure 1 Sliced snapshots of microstructure showing the system configuration of (a) top and (b) offset impact of second particles; color coding—light blue (bcc), green (twin), red (surface), dark blue (disordered).

Pressure, temperature, and strain evolution

- Rigorous deformation is observed for both top and offset impact.
- For the case of top impact, jetting was initiated by pressure wave propagation and evenly distributed at the particle-particle interface at a time of 4 ns. A localized thermal spike was also observed following jet initialization.
- For the case of offset impact, the second particle was firstly interacted with the first particle. At this stage, jetting was initiated at around 10 ns but distributed unevenly at the particle-particle interface. The thermal spike also occurred mostly on one side only. As the second particle reached to the substrate, the pressure wave was interacted with the substrate, and the jetting and the thermal spike were continuously formed at the particle-substrate interface at a time of around 20 ns.
- The different deformation behaviors for the cases of top and offset impact are also observed in the strain distribution analysis. For top impact, the first particle was severely deformed, and the strain was shown close to the particle-particle interface. On the other hand, during the offset impact, the deformation of the first particle was less than the one cased by top impact. Furthermore, the largest shear strain was observed at the particle-substrate interface during the offset impact.

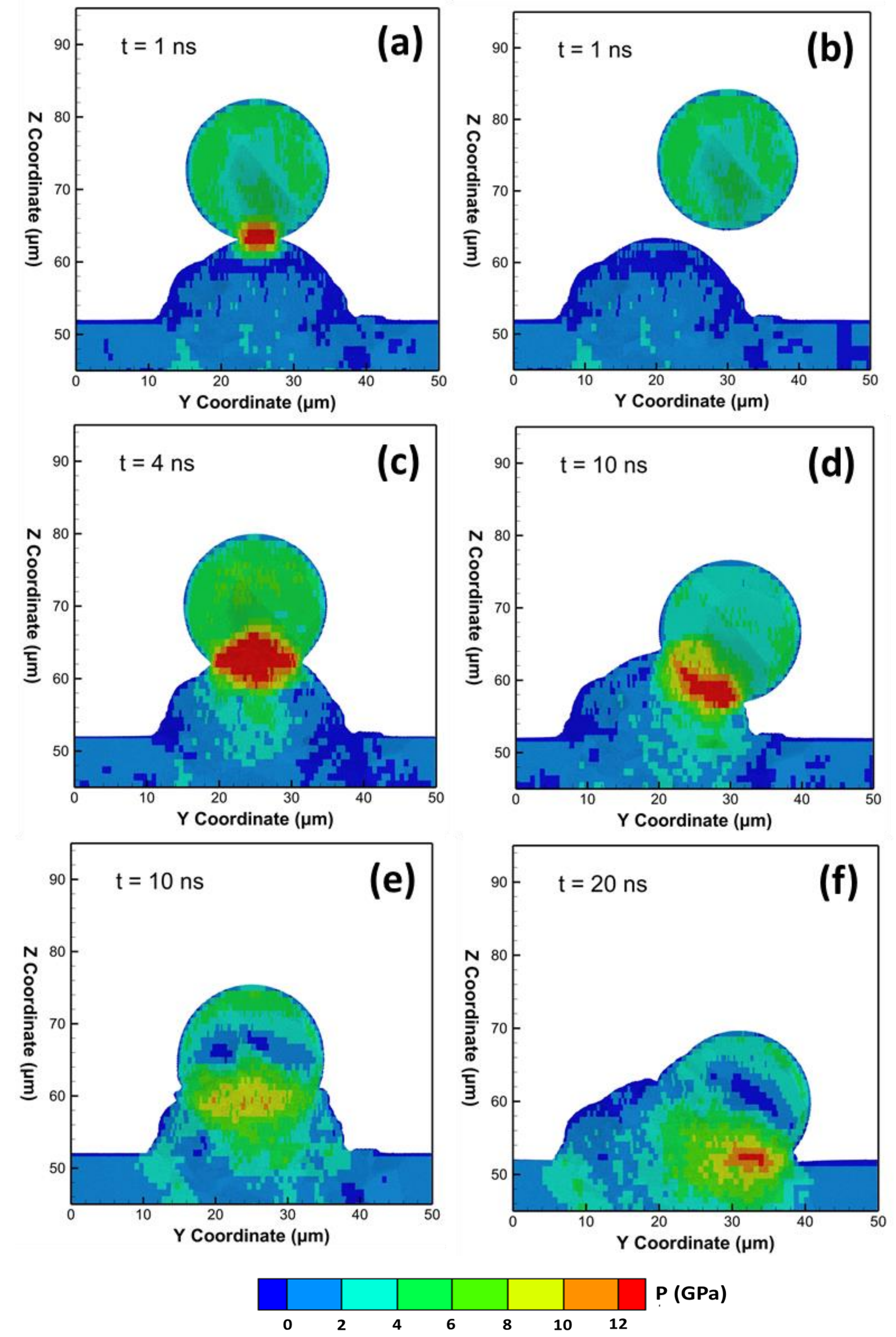

Figure 2 Pressure evolution for the cases of (a, c, e) top and (b, d, f) offset impact at (a, b) 1 ns, (c) 4 ns, (d, e) 10 ns, and (f) 20 ns after impact.

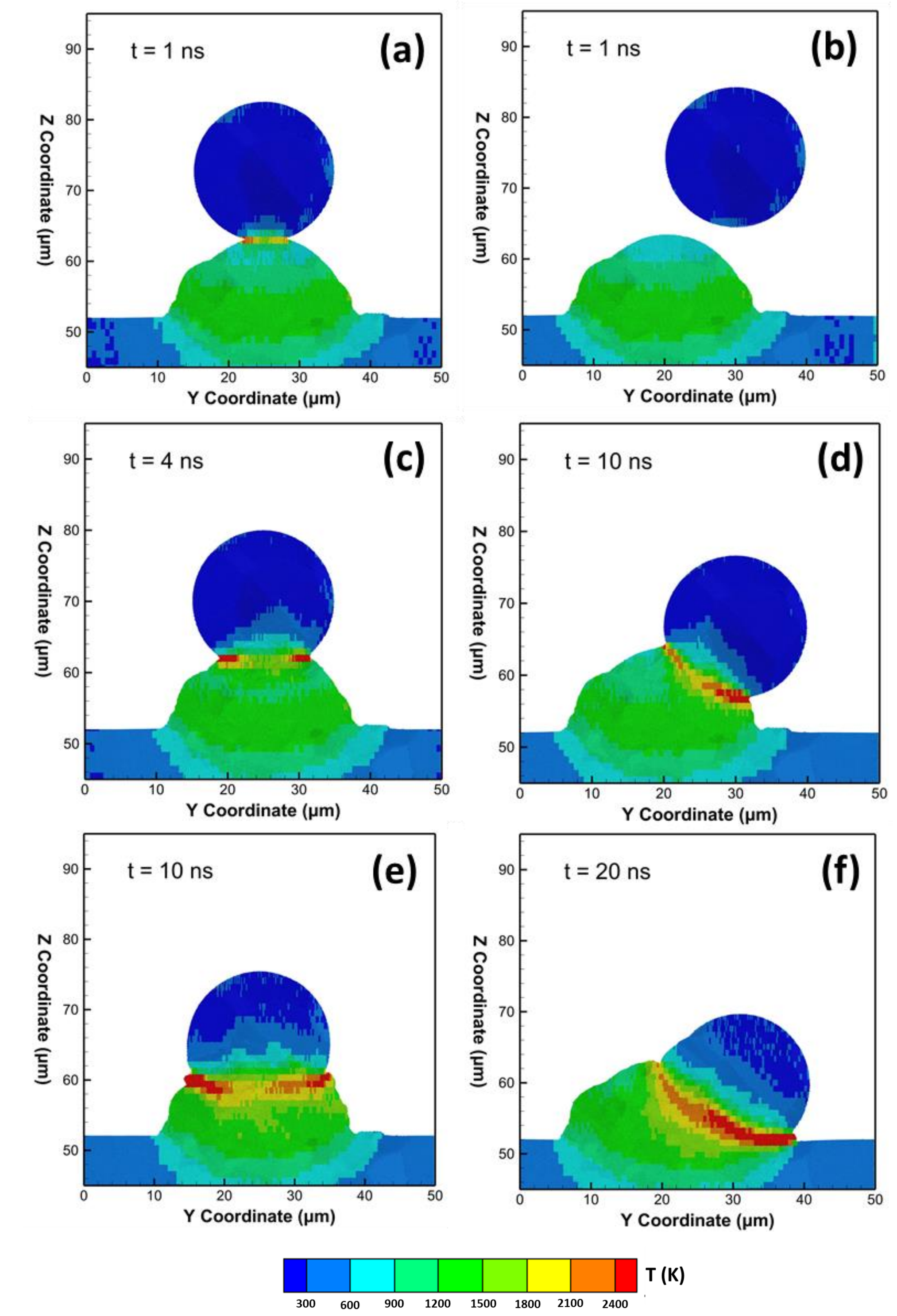

Figure 3 Temperature evolution for the cases of (a, c, e) top and (b, d, f) offset impact at (a, b) 2 ns, (c) 4 ns, (d, e) 10 ns, and (f) 20 ns after impact.

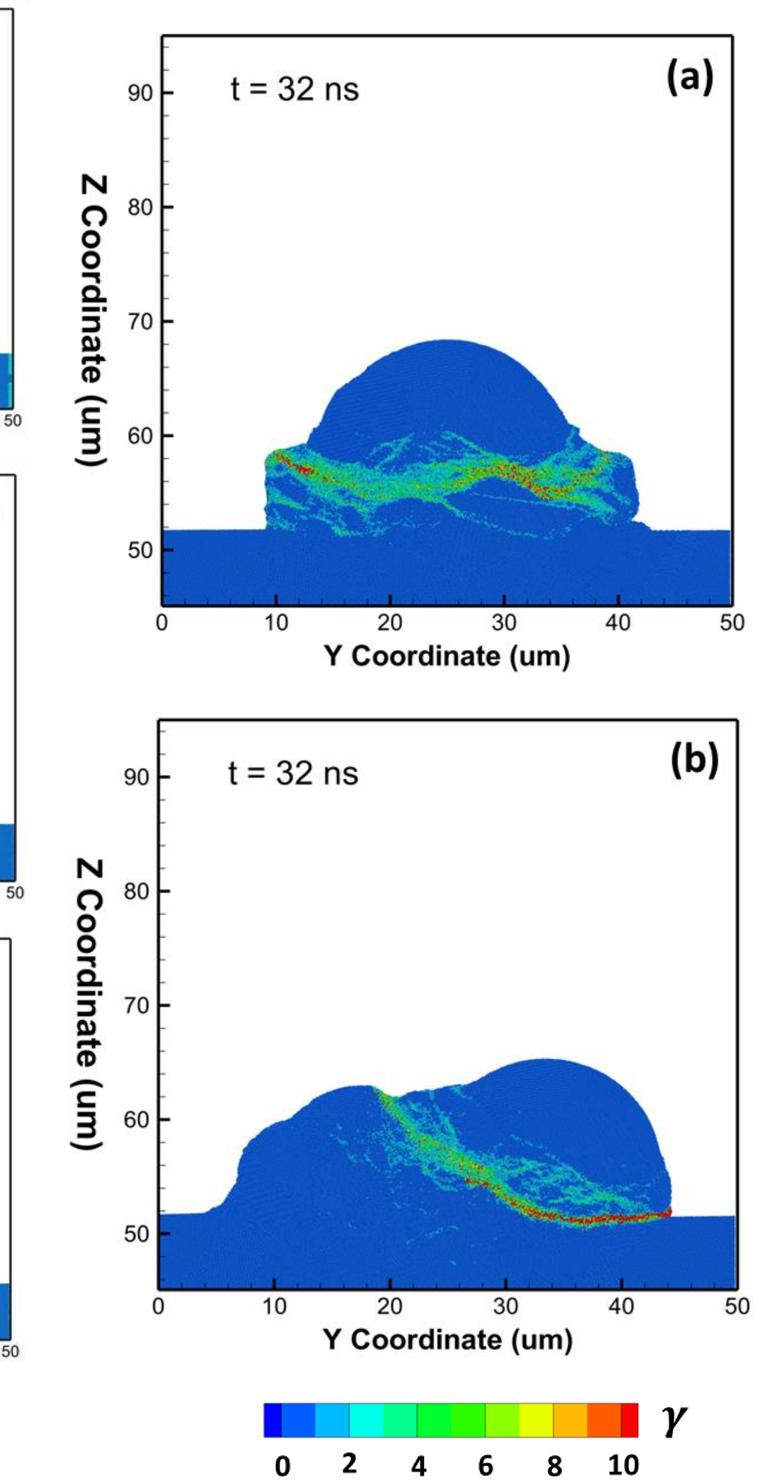

Figure 4 Strain distribution for the cases of (a) top and (b) offset impact at 32 ns after impact.

Microstructure and recrystallization

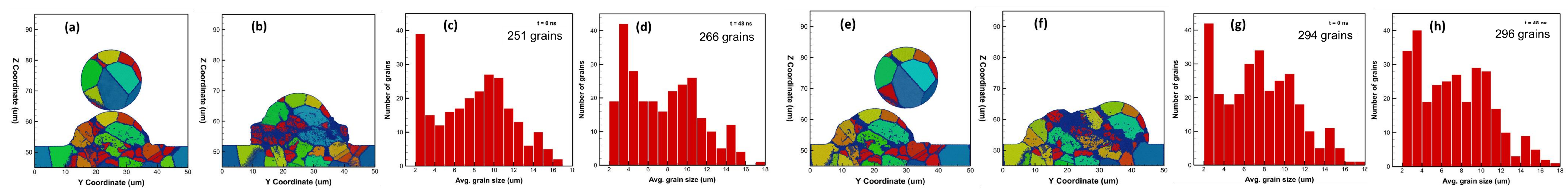

Figure 5 microstructure snapshots of a grain orientation representation and the corresponding grain size distribution for the cases of (a-d) top and (e-h) offset impact. For the case of top impact, the grain orientation representation and grain size distribution (a, c) before impact and (b, d) at 48 ns after impact. For the case of offset impact, the grain orientation representation and grain size distribution (e, g) before impact and (f, h) at 48 ns after impact.

Conclusions

- Cold spray multi-particle impact of Tantalum powders are modeled using QCGD simulations.
- Jetting is observed in the both cases of top and offset impact.
- For the case of top impact, severe deformation and jetting are evenly formed, accompanying with the localized thermal softening, at the particle-particle interface.
- For the case of offset impact, the second particle at the start is impacted on the first particle, initializing jetting and localized high temperature regions at a part of the particle-particle interface. When the second particle reaches to the substrate, the pressure wave starts to interact with the substrate and generate jetting as well as thermal spikes at the particle-substrate interface.
- Recrystallization is observed in the both impact cases. For top impact, the number of grains in the system is increased from 251 to 266 after impact, and the average grain size goes down from 8.15 to 7.79 µm. For the case of offset impact, recrystallization is not as obvious as in top impact. The number of grains almost remains the same after impact, and the average grain size only slightly decreases from 7.71 to 7.58 µm.

Reference

[1] A. M. Dongare, *Phil. Mag.* **94**, 3877 (2014).

[2] R. Ravelo et al. *Physical Review B* **88**(13), 134101 (2013).

Acknowledgments:

This material is based upon work supported by the U. S. Army Research Laboratory under contract/grant number W911NF-15-2-0026. Any opinions, findings, and conclusions or recommendations expressed in this publication are those of the author(s) and do not necessarily reflect the views of the U. S. Army Research Office or of the U. S. Government.

PI Contact:

- Avinash M. Dongare (dongare@uconn.edu)

Student Contact:

- Ching Chen (ching.chen@uconn.edu)